Continuum drift kinetics in NIMROD

E. Held and NIMROD Team.

CEMM at APS-DPP, Providence, RI 2012

Improved continuum algorithm I.

- Added F_{hot} data structure and advance for hot particles.
- Consolidated integrand routines to solve

$$
\begin{aligned}
&\partial_t f + (\mathbf{v}_{||} + \mathbf{v}_D)\cdot\nabla f \\
&+ \frac{s}{2}\Big[-(\mathbf{v}_{||} + \mathbf{v}_D)\cdot\nabla \ln T_0 - (1-\xi^2)\frac{\mathbf{b}}{B}\cdot\nabla\times\mathbf{E} + \\
&\frac{e}{s^2 T_0}(\mathbf{v}_{||} + \mathbf{v}_d)\cdot\mathbf{E} + (1+\xi^2)\frac{\mathbf{E}\times\mathbf{B}}{B^2}\cdot\nabla\ln B\Big]\frac{\partial f}{\partial s} \\
&+ \frac{1-\xi^2}{2\xi}\Big[-(\mathbf{v}_{||} + \mathbf{v}_d)\cdot\nabla\ln B + \xi^2\frac{\mathbf{b}}{B}\cdot\nabla\times\mathbf{E} + \\
&\qquad \frac{e}{s^2 T_0}(\mathbf{v}_{||} + \mathbf{v}_d)\cdot\mathbf{E} + \xi^2\frac{\mathbf{E}\times\mathbf{B}}{B^2}\cdot\nabla\ln B\Big]\frac{\partial f}{\partial \xi} = C(f)
\end{aligned}
$$

for F_e, F_i and F_h.

Improved continuum algorithm II.

- Added $\partial B/\partial t$ in acceleration and $\partial_t \mathbf{b}$ in $\mathbf{v}_D$ and $\mathbf{v}_d$:

$$\mathbf{v}_D = \frac{\mathbf{E}\times\mathbf{B}}{B^2} + \frac{\rho_0 v_0 s^2}{2B}\left(1+\xi^2\right)\mathbf{b}\times\nabla\ln B + \frac{\rho_0 v_0 s^2}{B}\xi^2\mu_0\mathbf{J}_\perp + \frac{\rho_0 v_0 s^2}{2B}(1-\xi^2)\mu_0\mathbf{J}_{||} + \rho_0 s\xi\mathbf{b}\times\partial_t\mathbf{b}$$

$$\mathbf{v}_d = \mathbf{v}_D - \frac{\mathbf{E}\times\mathbf{B}}{B^2} + \frac{\rho_0 v_0 s^2}{2B}\left(1+\xi^2\right)\mathbf{b}\times\nabla\ln B$$

Improved continuum algorithm III.

- Generalized mapping between logical and pitch-angle space for 1D finite elements: $\frac{v_{||}}{v} = \sum_i (\frac{v_{||}}{v})_i \phi_i(x)$.
- Option for adding pre-assigned nodes into s grid.

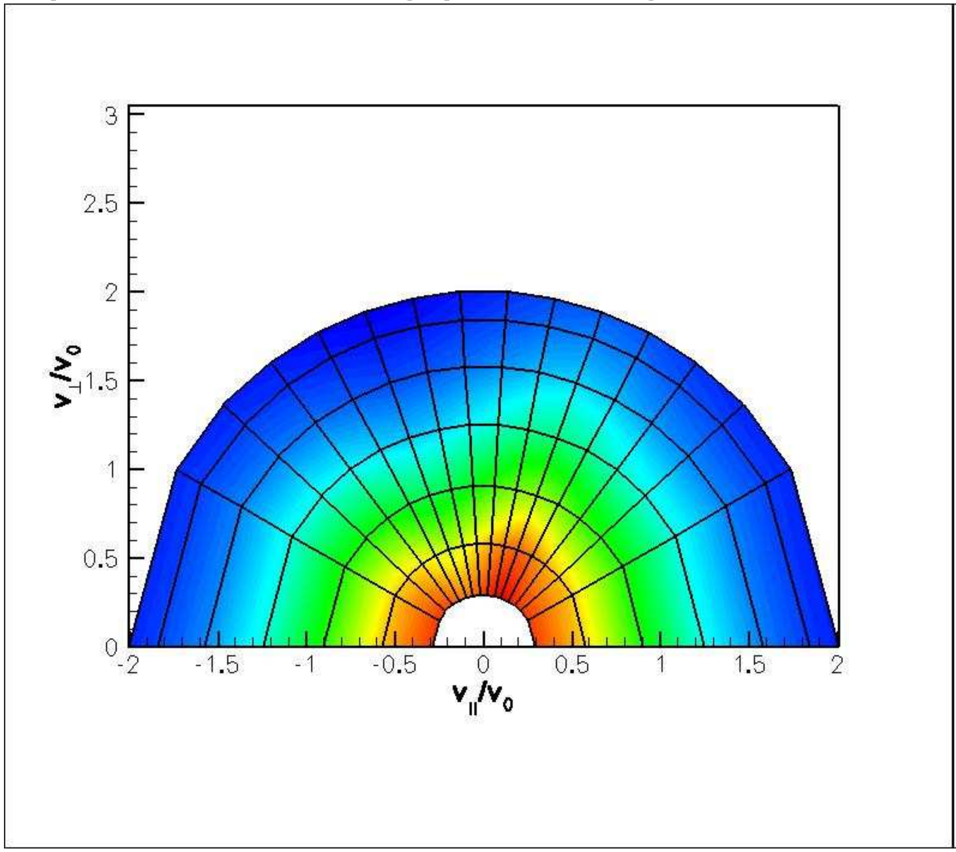

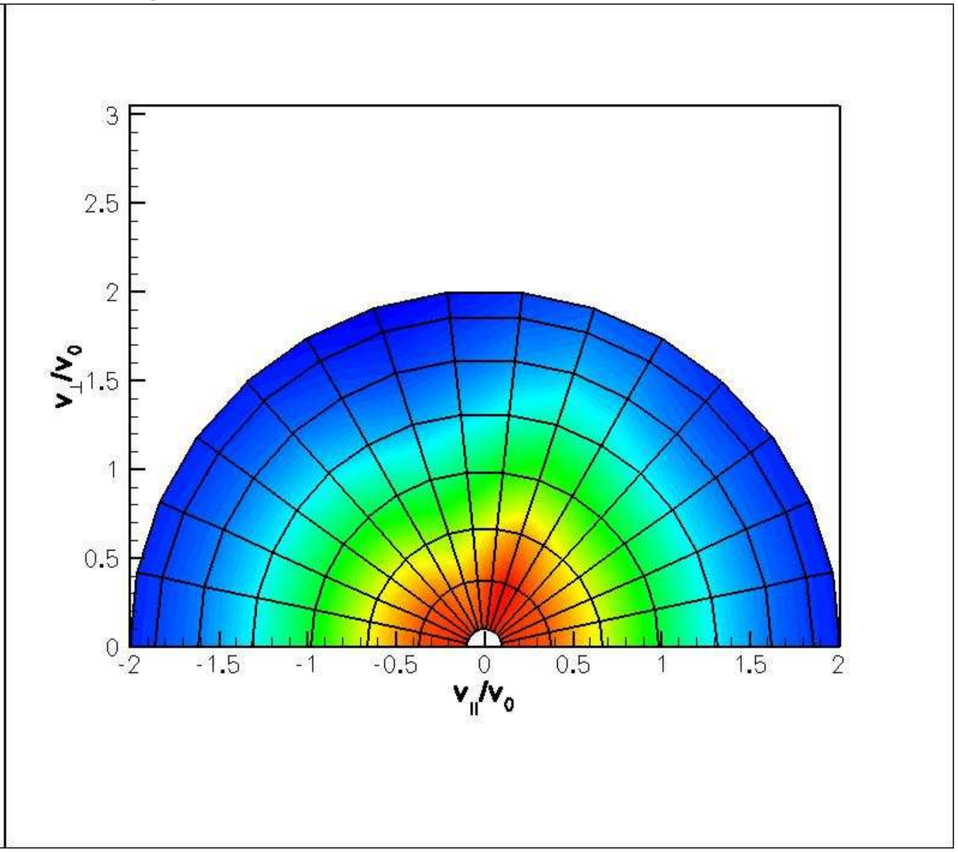

δf PIC approach I for hot particle kink benchmark.

- Evolve δf for hot, drifting, minority ion species as in C. C. Kim, *Phys. Plasmas* **15**, 072507 (2008):

$$\frac{\delta f}{f_0(P_\zeta)} = \left\{ \frac{mRB_\phi}{e\psi_n B^3}\left[\left(v_{||}^2 + v_\perp^2/2\right)\delta\mathbf{B}\cdot\nabla B - \mu_0 v_{||}\mathbf{J}\cdot\mathbf{E}\right] + \frac{1}{\psi_n}\left(\mathbf{E}\times\mathbf{B}/B^2 + v_{||}\delta\mathbf{B}/B\right)\cdot\left(\nabla\psi_p - mv_{||}\nabla(RB_\phi)/(qB)\right) + \frac{3}{2}\frac{e\epsilon^{1/2}}{\epsilon^{3/2}+\epsilon^{3/2}}\mathbf{v}_D\cdot\mathbf{E}\right\}$$

- In original, NIMROD δf PIC calculation, slowing down distribution, $f_0(P_\zeta,\epsilon) = P_0\exp(P_\zeta/\psi_n)/(\epsilon^{3/2}+\epsilon_c^{3/2})$ was used in weight equation but $f_0(\psi,\epsilon) = P_0\exp(\psi/\psi_n)/(\epsilon^{3/2}+\epsilon_c^{3/2})$ was used when taking moments: $\delta p_\perp = \int d\mathbf{v}\mu B\frac{\delta f}{f_0(P_\zeta)}f_0(\psi)$ and $\delta p_{||} = \int d\mathbf{v}v_{||}^2\frac{\delta f}{f_0(P_\zeta)}f_0(\psi)$.

Continuum results sensitive to f_0.

- Continuum approach predicts different growth rates and real frequences when using $f_0(\psi, \epsilon)$ versus $f_0(P_\zeta, \epsilon)$ in moments.

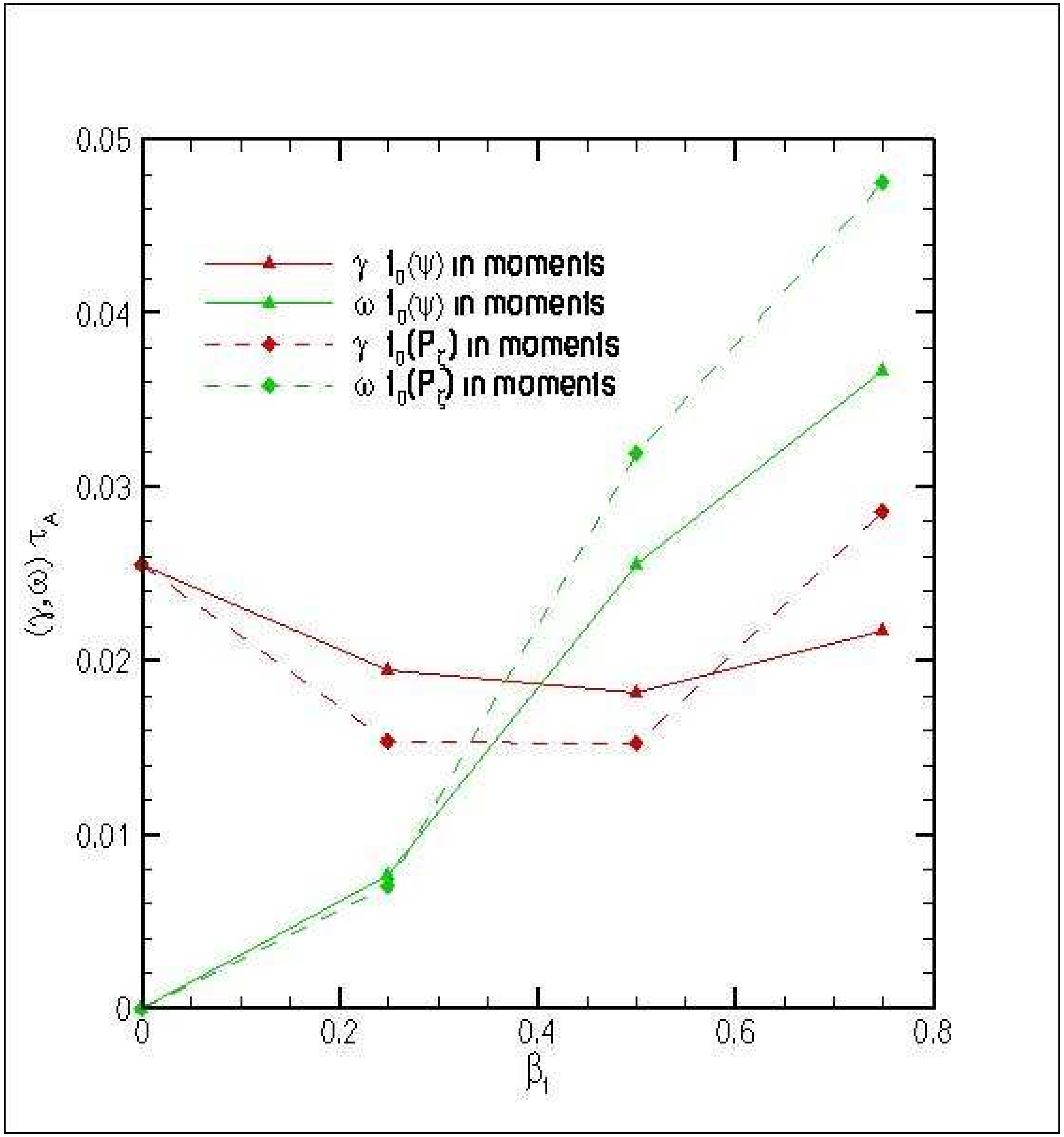

δf PIC approach II for hot particle kink benchmark.

- Fu's approach (*Phys. Plasmas* **13**, 052517 (2006)) with M3D used:
  $f_0(\psi,\epsilon) = P_0 \exp(\langle\psi\rangle/\psi_n)/(\epsilon^{3/2}+\epsilon_c^{3/2})$,
  where
  $\langle\psi\rangle = P_\zeta/e - \frac{m}{e}\langle v_{||} R \frac{B_\phi}{B}\rangle \approx P_\zeta/e$
  for trapped particles and
  $\langle\psi\rangle = P_\zeta/e - \frac{m}{e}\langle v_{||} R \frac{B_\phi}{B}\rangle \approx P_\zeta/e - vR_0 sign(\frac{v_{||}}{v})\sqrt{1-\mu B_0/\epsilon}$
  for passing particles.
- Here ψ_n used to match shape of MHD pressure profile and P_0 used to replace fraction of MHD pressure at magnetic axis.

Comparison of Kim's and Fu's f_0.

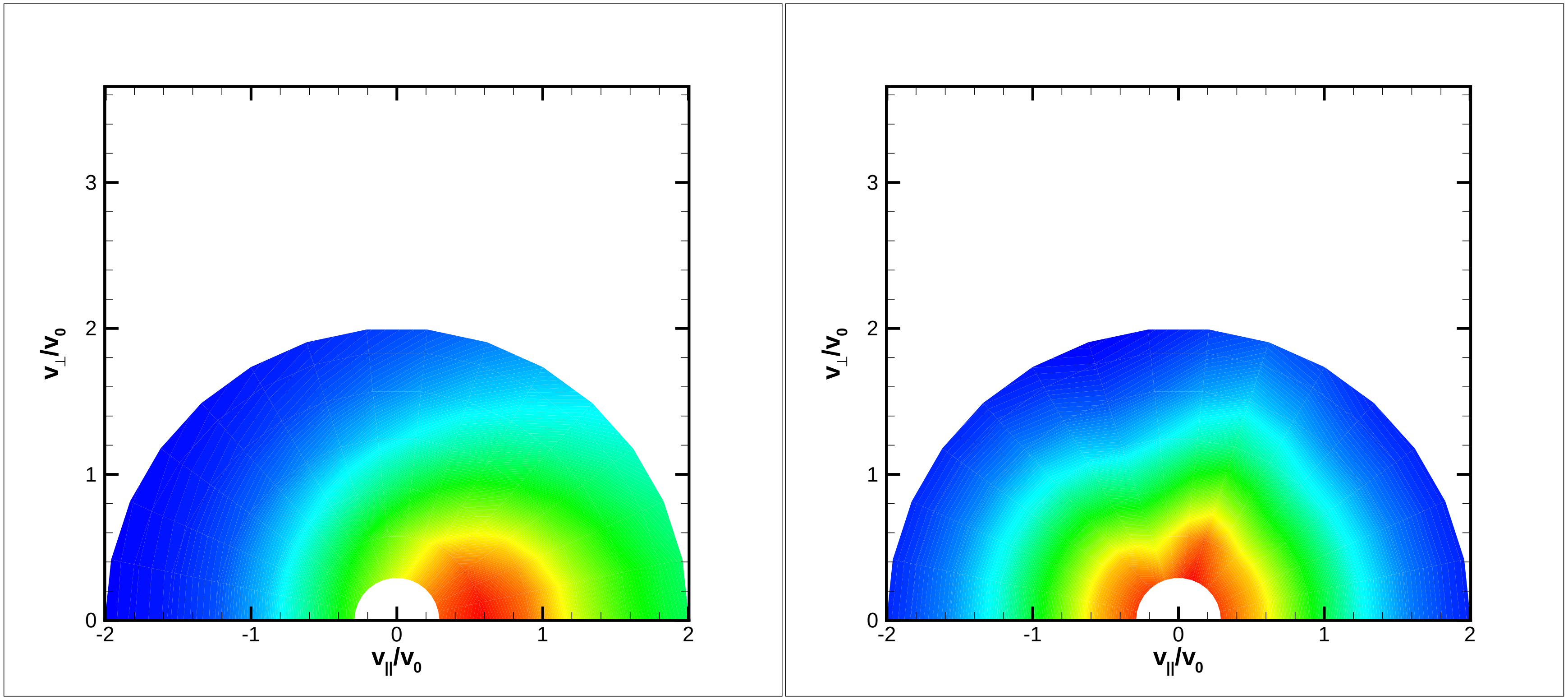

With Fu's f_0, continuum method agrees with δf PIC.

- Increasing hot particle pressure first stabilizes and then destabilizes mode.
- Growth rates and real frequencies similar.

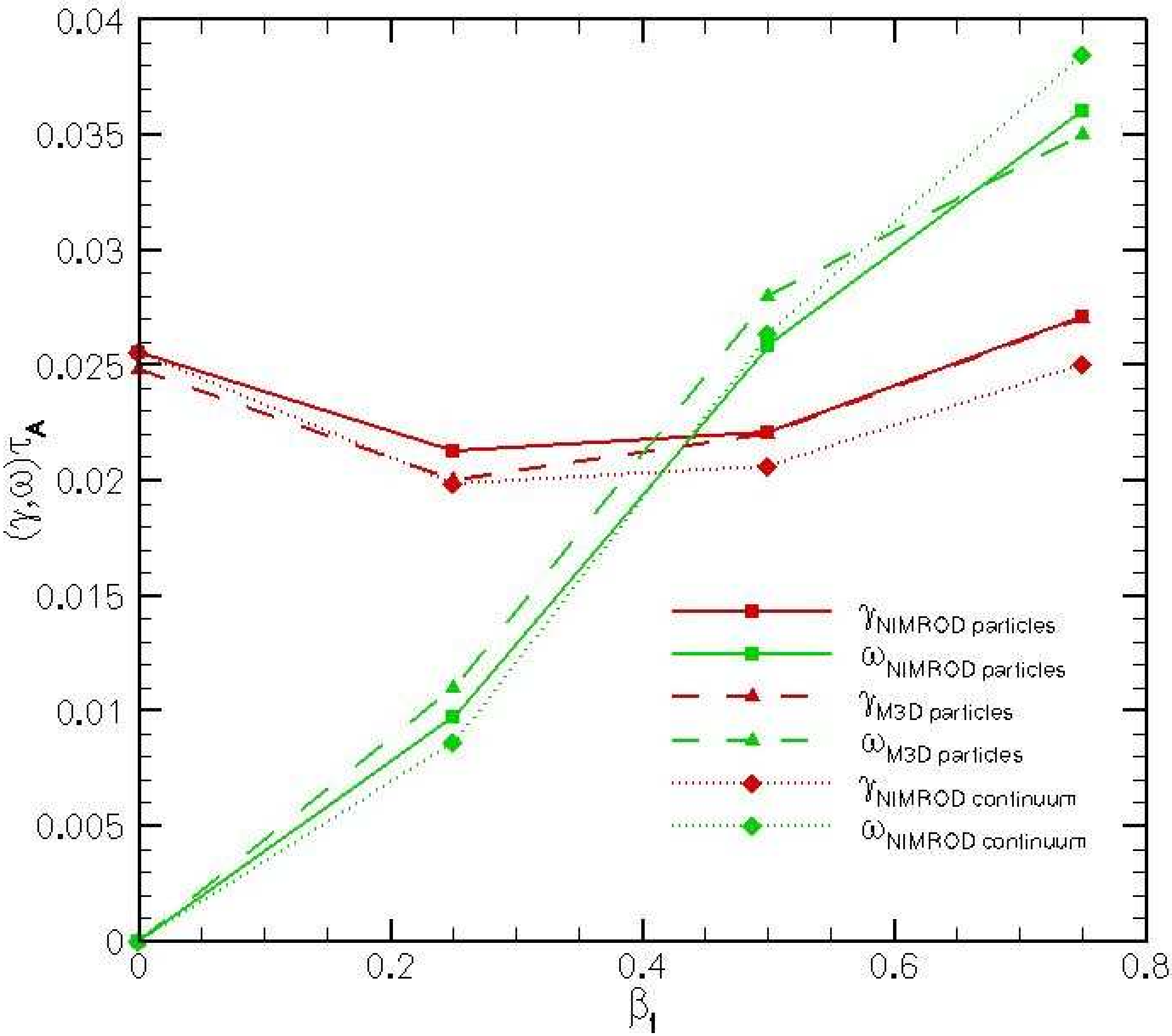

Vertex nodes in ξ grid at $\pm\xi_t(\psi)$ help convergence.

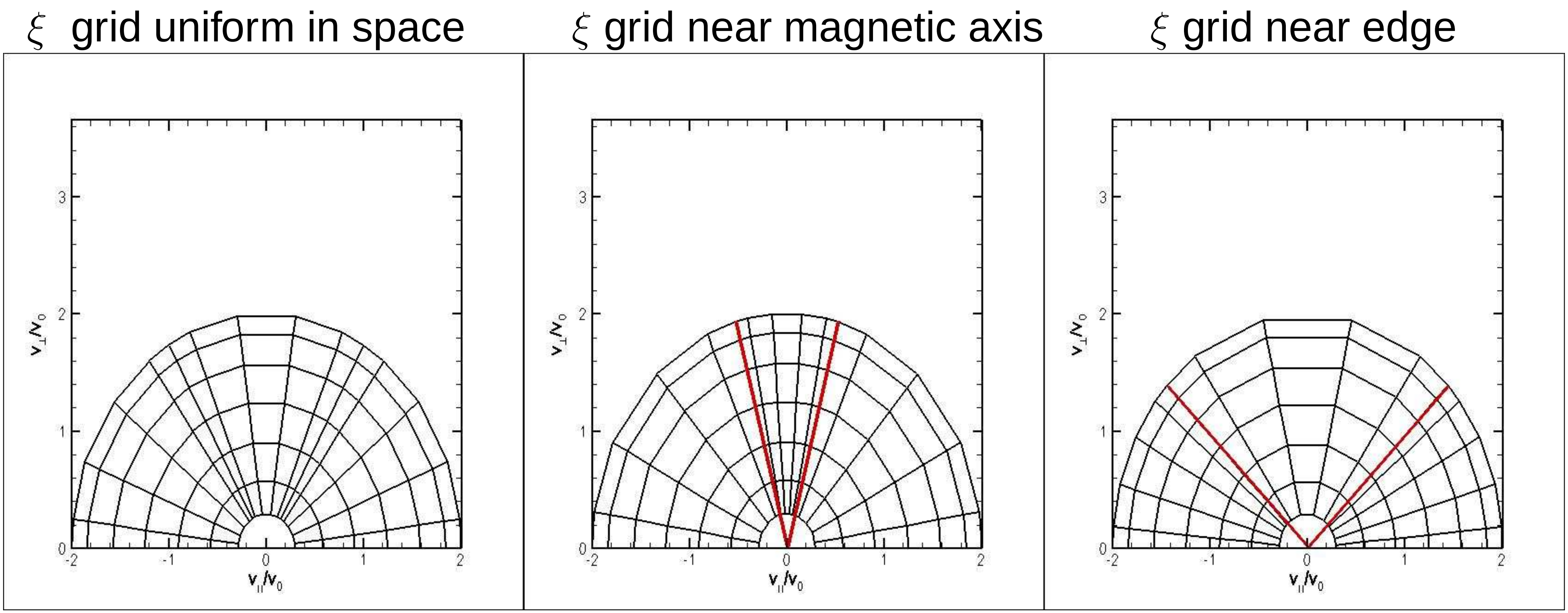

Growth rate convergence

vertex nodes uniform in $cos^{-1}(\xi)$

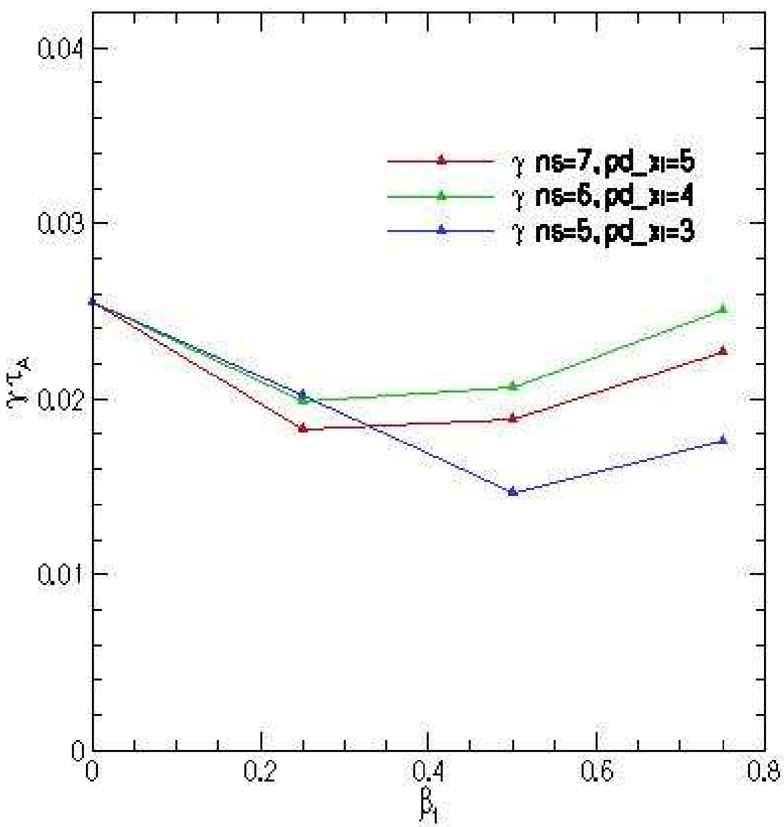

vertex nodes at $\pm\xi_t(\psi)$

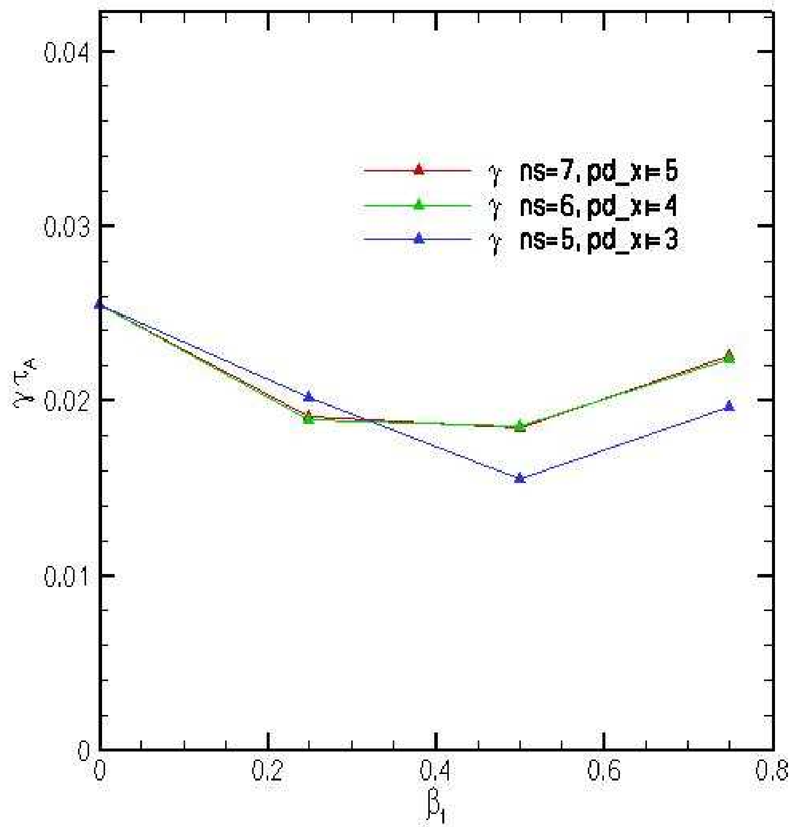

Real frequency convergence.

vertex nodes uniform in $cos^{-1}(\xi)$

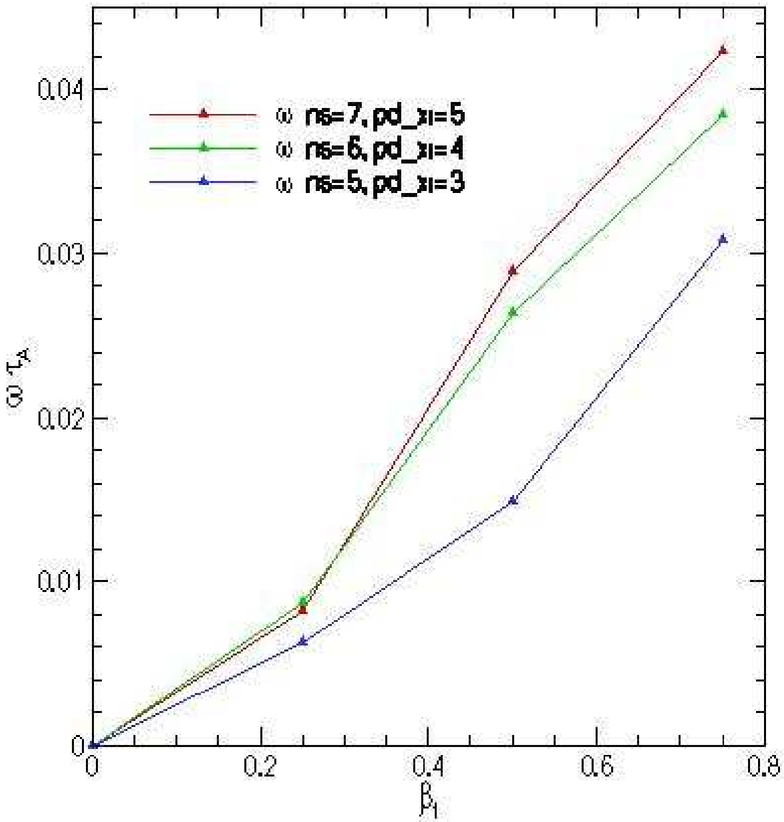

vertex nodes at $\pm\xi_t(\psi)$

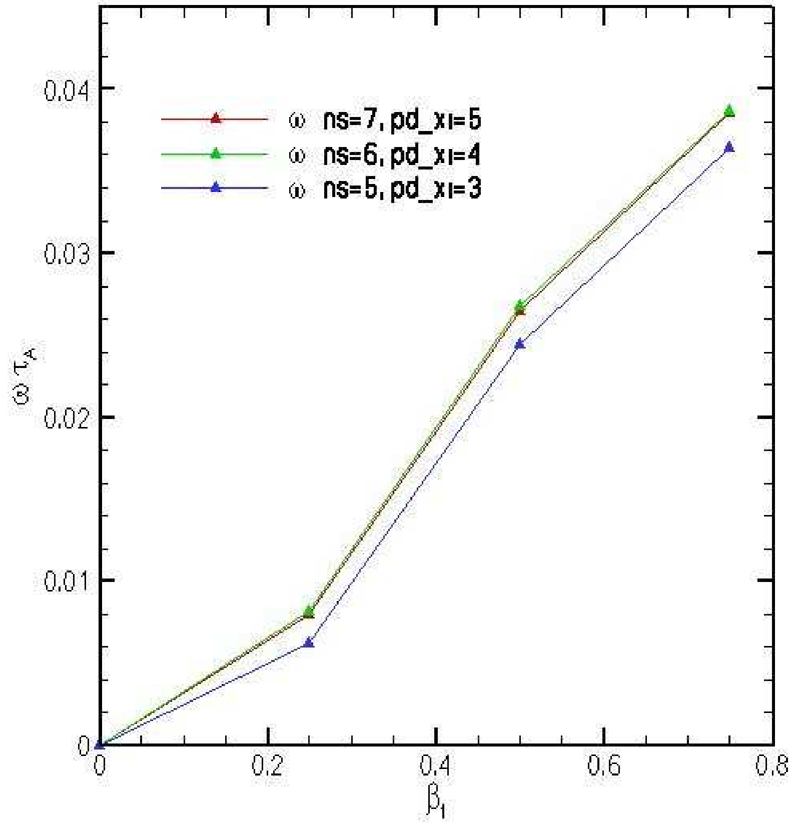

Trapped particles dominate anisotropic pressure response.

- Anisotropic hot particle pressure shifted to outboard side of torus.

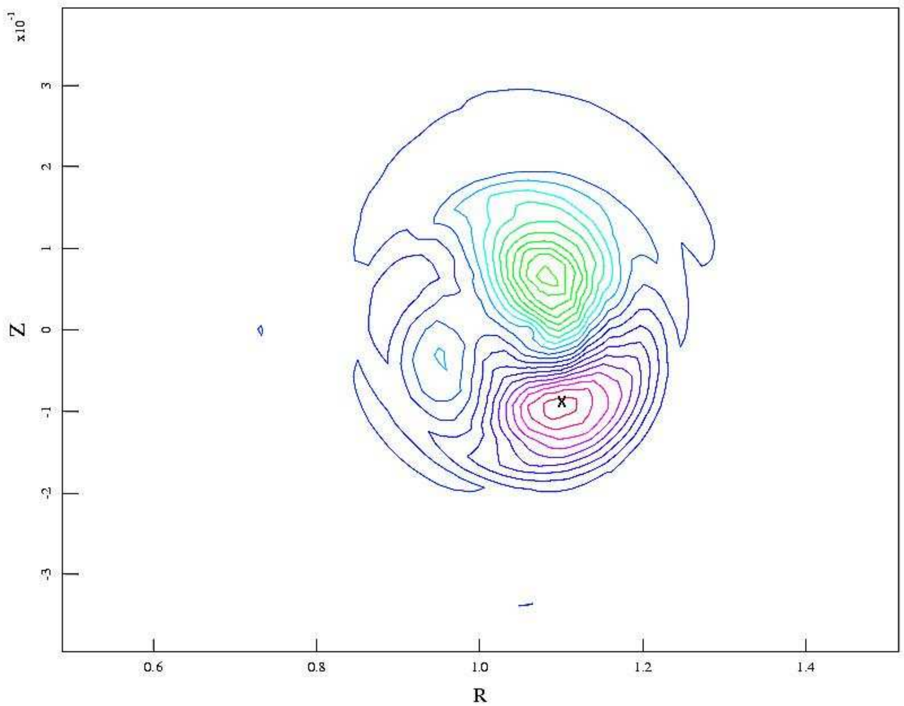

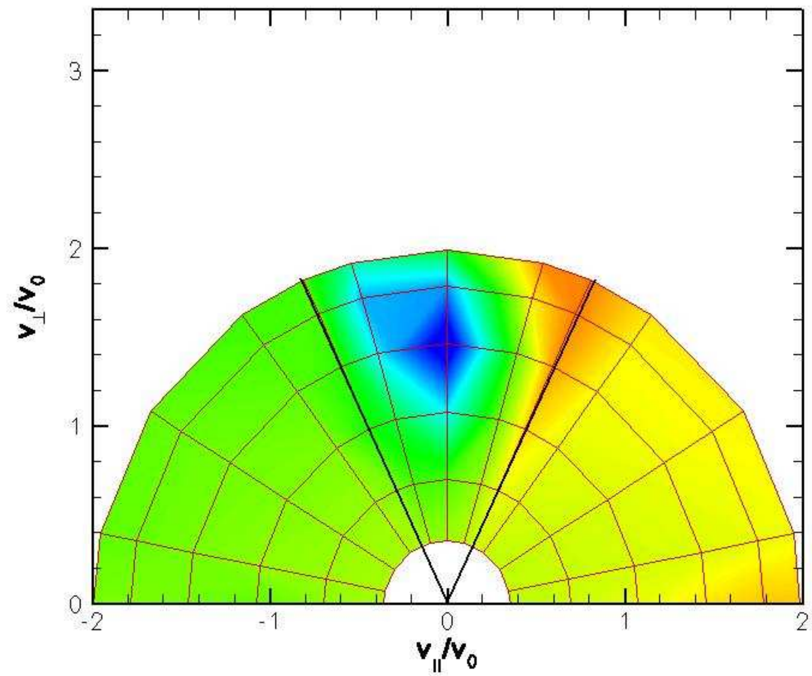

Future applications for continuum drift hot particles, ions and electrons in NIMROD.

- ITG validation exercise. Compare second-order continuum drift kinetics for bulk ions with kinetic and fluid analytics and numerics. Schnack with CU, Tech-X and USU.
- Giant Sawtooth. High-energy tail coded up and computations with DIII-D equilibria underway.
- Reversed Shear Alfven Eigenmode (RSAE) verification and validation (Spong, *et al.*), TAEFL, GTC and GYRO codes.
- Neoclassical tearing modes with RF quasilinear operator in electron drift kinetic equation. SWIM-related work with Jenkins and Kruger at Tech-X.